Korean J. Chem. Eng., 36(10), 1732-1739 (2019)
DOI: 10.1007/s11814-019-0374-z

pISSN: 0256-1115
eISSN: 1975-7220

Effect of temperature on the performance of aqueous redox flow battery using carboxylic acid functionalized alloxazine and ferrocyanide redox couple

Cheunho Chu, Byeong Wan Kwon, Wonmi Lee, and Yongchai Kwon†

Graduate School of Energy and Environment, Seoul National University of Science and Technology,
232 Gongneung-ro, Nowon-gu, Seoul 01811, Korea
(*Received 16 July 2019 • accepted 22 August 2019*)

Abstract−Carboxylic acid functionalized alloxazine (alloxazine-COOH) and ferrocyanide are utilized as active species for aqueous redox flow battery (ARFB), and the effect of operating temperature on the performance of ARFB was investigated. Based on electrochemical characterization, although ferrocyanide is in a quasi-reversible state at room temperature, the state becomes irreversible as temperature increases. By the use of carbon felt (CF) containing carbon-oxygen functional groups, the activity of ferrocyanide is enhanced without side effect, such as irreversible redox reactivity. This is because the hydrophilic (charge-dipole) interaction between dipole groups (hydroxyl and carbonyl groups) onto CF and ferricyanide ions promotes the oxidation reaction of ferricyanide. Though alloxazine-COOH coated on glassy carbon electrode shows irreversible state compared to ferrocyanide as temperature increases, the activity of alloxazine-COOH is also enhanced by using the hydrophilic group doped CF. To prove whether the redox reactivity of the two active species is improved with increase in temperature, the performance of ARFBs using them was evaluated in the different temperature conditions. When the temperature of both anolyte and catholyte is 45 °C, average discharge capacity and state of charge are 24 Ahr·L^{-1} and 90%, and the values are reduced to 23 Ahr·L^{-1} and 86% in ARFB of only catholyte heating, 22 Ahr·L^{-1} and 82% in ARFB of only anolyte heating and 21.3 Ahr·L^{-1} and 80% with no heating. Based on that, it is speculated that the operation temperature can be a factor in determining the performance of ARFB.

Keywords: Alloxazine-COOH, Ferrocyanide, Aqueous Organic Redox Flow Battery, Redox Reaction Rate, Temperature Effect

INTRODUCTION

Renewable energy, such as solar, wind, and wave power, is a very useful resource because it is sustainable and ecofriendly. However, utilization has an obvious limitation because of their intermittent generation. Therefore, many researchers have attempted to overcome the drawback of renewable energy sources using energy storage system (ESS). The ESS can store and convert the electrical energy to the chemical energy and vice versa, while there are various ESS options, such as capacitor, supercapacitor, flywheel energy storage, lead-acid battery, redox flow battery, and lithium-ion battery [1-7].

Among them, the redox flow battery (RFB) is widely considered as one of the appropriate ESSs due to the advantages such as long calendar life, excellent system scalability, and proper flexibility. The most attractive point is that this RFB can use two external tanks for storing active species, and its energy density can be determined by controlling tank size [8-10]. In spite of that, the main components for operating RFB, such as membrane, electrode, catalyst, and redox couple, should be further developed [11-18]. Selecting the proper redox couple is the most important because the performance and stability of RFB mainly depend on how the redox couple is decided. Of the redox couple candidate, to date, the all-vanadium redox flow battery (VRFB) has been in the spotlight because this alleviates the crossover problem by employing the same vanadium element for anolyte and catholyte, and has an excellent cell potential of 1.259 V and a proper level of sulfuric acid solubility utilized as supporting electrolyte [19-21].

However, the VRFB still has shortcomings. First, the vanadium is rare and very expensive, and is only reserved in the limited regions [22]. Second, the available temperature range of VRFB is very narrow, meaning that V^{3+} and V^{5+} ions can be precipitated at temperatures outside 10-40 °C [23]. Third, the redox reactivity of V^{4+}/V^{5+} reaction is relatively low. Thus, the use of catalysts to promote the slow reaction is essentially required and leads to an increase in cost [24]. Fourth, in the case of V^{2+}/V^{3+} reaction, the way to suppress hydrogen evolution reaction (HER) should be considered because the two reactions occur at a similar potential. For that, catalysts and additives for controlling HER are needed [25,26].

As an alternative to VRFB, aqueous organic materials can be considered because they have the merit of low cost, scalability, good biodegradability, excellent structural diversity, and abundant amount in nature [27]. So far, many candidates of aqueous organic material have been applied as the redox couple replacing vanadium, and the aromatic compounds, such as aza functional group, alloxazine, ferrocyanide, ferrocene, and methyl viologen, are one group of them [28-30].

In this study, we used the alloxazine derivative and ferrocyanide as catholyte and anolyte, respectively. The alloxazine has advantages like proper aqueous solubility, excellent safety and desirable poten-

†To whom correspondence should be addressed.
E-mail: kwony@seoultech.ac.kr
Copyright by The Korean Institute of Chemical Engineers.

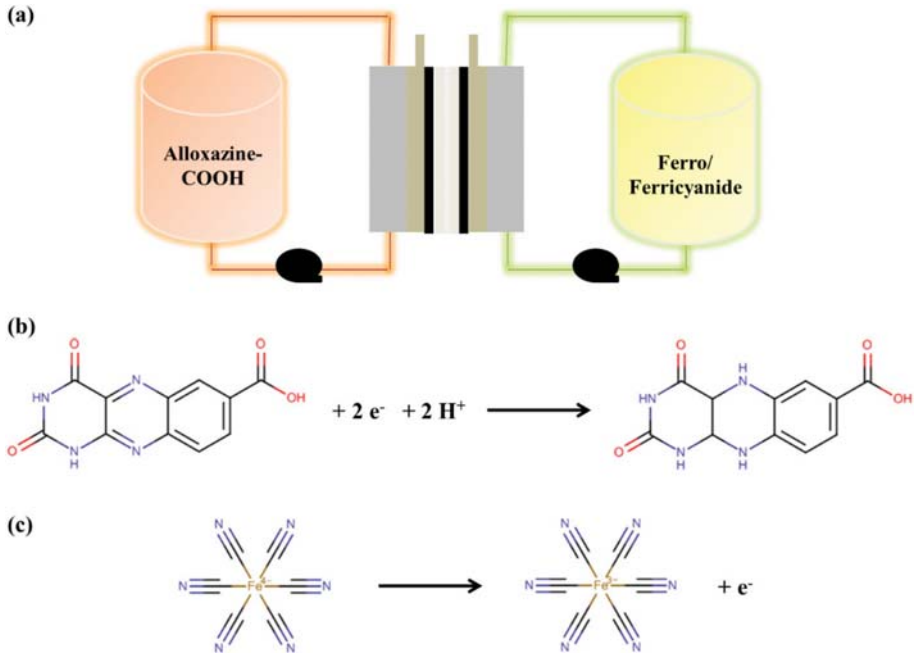

Fig. 1. Schemes showing (a) the ARFB full cell structure and the redox reactions of (b) alloxazine-COOH and (c) ferrocyanide.

tial value as catholyte, and is further modified by carboxylic acid (COOH) to increase aqueous solubility (alloxazine-COOH) [29,31]. On the other hand, ferrocyanide can offer advantages like excellent alkali-based aqueous solubility and favorable potential value as anolyte [32].

Aqueous organic RFB (AORFB) using alloxazine-COOH and ferrocyanide as redox couple was already suggested with excellent performance. However, there have been no previous reports representing the effect of operating temperature on the performance of AORFB using this redox couple, although the temperature is an important parameter to affect the performance of AORFB [29,31]. Thereby, in this study, we first investigated how the performance of AORFB is affected by the operating temperature and this is the major originality of this study. Fig. 1 shows the scheme of AORFB using alloxazine-COOH and ferrocyanide as redox couple and the redox reaction sequence of alloxazine-COOH and ferrocyanide.

EXPERIMENTAL

1. Materials

To prepare the catholyte and anolyte consisting of alloxazine-COOH and ferrocyanide, 3,4-dimaninobenzoic acid and alloxan monohydrate were purchased from Alfa Aesar. Acetic acid and boric acid were from Sigma Aldrich. Potassium hexacyanoferrate(II) trihydrate and potassium ferricyanide (III) were also from Sigma Aldrich. Potassium hydroxide (95.0%) that was used for supporting electrolyte solution was obtained from Samchun Chemical.

2. Synthesis of Alloxazine-COOH

To synthesize alloxazine-COOH, 3.04 g (20 mmol) of 3,4-diaminobenzoic acid was dissolved in 170 mL of acetic acid with stirring, and then 1.36 g (22 mmol) of boric acid and 3.36 g (21 mmol) of alloxan monohydrate were further added. The entire solution was stirred for 3 h at room temperature. After the process, precipitated product was filtered off and washed, first with 50 mL of acetic acid and then with 50 mL of diethyl ether (purchased by Sigma Aldrich), 100 mL of de-ionized (DI) water, and last 50 mL of diethyl ether.

3. Electrochemical Measurements

3-1. Half-cell Electrochemical Characterization

To evaluate the electrochemical properties of alloxazine-COOH and ferrocyanide, cyclic voltammogram (CV) curves were measured in three electrode cells using a potentiostat (SP-240, BioLogic). Here, Pt wire and Ag/AgCl were used as counter and reference electrodes, respectively, and glass carbon electrode (GCE, 5 mm diameter, active area 0.196 cm^2) was considered as the working electrode. From the CV curves, the redox reactivity of alloxazine-COOH and ferrocyanide was investigated, and that of alloxazine and alloxazine-COOH at different temperatures (20, 35, and 45 °C) were compared. The scan rates used were 10 and 100 $mV \cdot s^{-1}$. As electrolyte, 0.01 M of both alloxazine-COOH and ferrocyanide that was dissolved into 20 mL of 1.0 M potassium hydroxide (KOH) solution was used.

2-2. AORFB Full Sell Measurements

For AORFB full cell tests, charge-discharge equipment (Wonatech, WBCS3000) was used. 0.5 M of the alloxazine-COOH was prepared in 2.5 M KOH solution as catholyte, and then the prepared solution filled a tank of the volume of 15 mL. 0.4 M of ferrocyanide was dissolved into 1 M KOH solution as anolyte, and it was filled a tank of volume of 56.3 mL. A carbon felt (XF30A, Toyobo, Japan) that was 3 mm thick was used as the electrode for AORFB full cell. The active area of the carbon felt used was 4 cm^2, while Nafion 117 membrane was used as separator. During charge and discharge steps, a current density of 100 $mA \cdot cm^{-2}$ was applied under the cut-off voltage ranges of 0.5-1.8 V for 100 cycles. To compare the performance of alloxazine and alloxazine-COOH at different

temperatures (20, 35, and 45 °C), the capacity and efficiency of the AORFB full cell were measured. To investigate the effect of operating temperature on the performance of AORFB, the following four different types of experiments were conducted: (i) heating of 45 °C in both anolyte and catholyte, (ii) heating of 45 °C only in anolyte, (iii) heating of 45 °C only in catholyte, and (iv) no heating.

RESULTS AND DISCUSSION

1. Evaluation of Electrochemical Characterization

According to the Arrhenius equation, temperature is an important parameter for determining chemical reaction, and in general, as temperature increases, reaction rate increases, and kinetic energy of active species becomes higher than their activation energy. Thus, increasing the operation temperature for ARFB can be a way to improve its performance [33]. To investigate how temperature affects the redox reactivity of active species, electrochemical evaluations were performed under different temperature conditions (20, 35, and 45 °C). At first, the effect of temperature on the redox reactivity of ferrocyanide was measured (Fig. 2). In terms of anodic and cathodic peak current densities (I_{pa} and I_{pc}), those of ferrocyanide measured at 45 °C were 2.79 and −2.33 mA cm^{-2}, while those at 20 °C were 2.15 and −2.06 mA cm^{-2}. This means that when the operating temperature increases, redox reactivity also improves. This is due to the improvements in the mobility and reaction rate of ferrocyanide by the increase in temperature. In addition, electrochemical reversibility and peak potential difference of ferrocyanide were measured at 45 °C are 1.2 and 0.072 V, respectively, while those at 20 °C were 0.96 and 0.050 V. This is explained as that the oxidation reactivity of ferrocyanide is more sensitive to temperature than its reduction reactivity. The difference between the reactivity is because ferricyanide has five unpaired electrons in d-orbital, while ferrocyanide that is a recued form of ferricyanide has no unpaired electron (Fig. 2(c)) [34,35]. Usually, the unpaired electrons belonging to transition metal can easily provide the electrons for ligand, such as water, to form a coordination bond. Thus, ferricyanide can interact with an aqueous solution like KOH, and its reactivity becomes higher than that of ferrocyanide [36,37]; since the redox reactivity generally increases as temperature increases, the solubility of ferricyanide will be proportional to temperature, while the tendency to be ferricyanide from ferrocyanide can be more activated. This result also indicates that the oxidation reaction of ferrocyanide for forming ferricyanide occurs more spontaneously as temperature increases. Namely, as temperature increases, the oxidation reaction rate of ferrocyanide is higher than its reduction reaction rate [38].

Next, to investigate the effect of temperature on the redox reactivity of alloxazine-COOH, its reaction kinetic parameters were measured (Fig. 3). As shown in Fig. 3, as temperature increased, the redox reactivity of alloxazine-COOH was improved. For instance, I_{pa} and I_{pc} measured at 45 °C were 1.201 and −1.976 mA cm^{-2}, and the values were 11.8% and 25.8% higher than those measured at 20 °C (I_{pa} and I_{pc} are 1.071 and −1.467 mA cm^{-2}). This indicates that the reduction reactivity of alloxazine-COOH is more sensitive to temperature than its oxidation reactivity. It is because the interaction of chemical bonds within alloxazine-COOH induces the changes in polarity and hydrogen bonding capabilities. Namely, the reduced

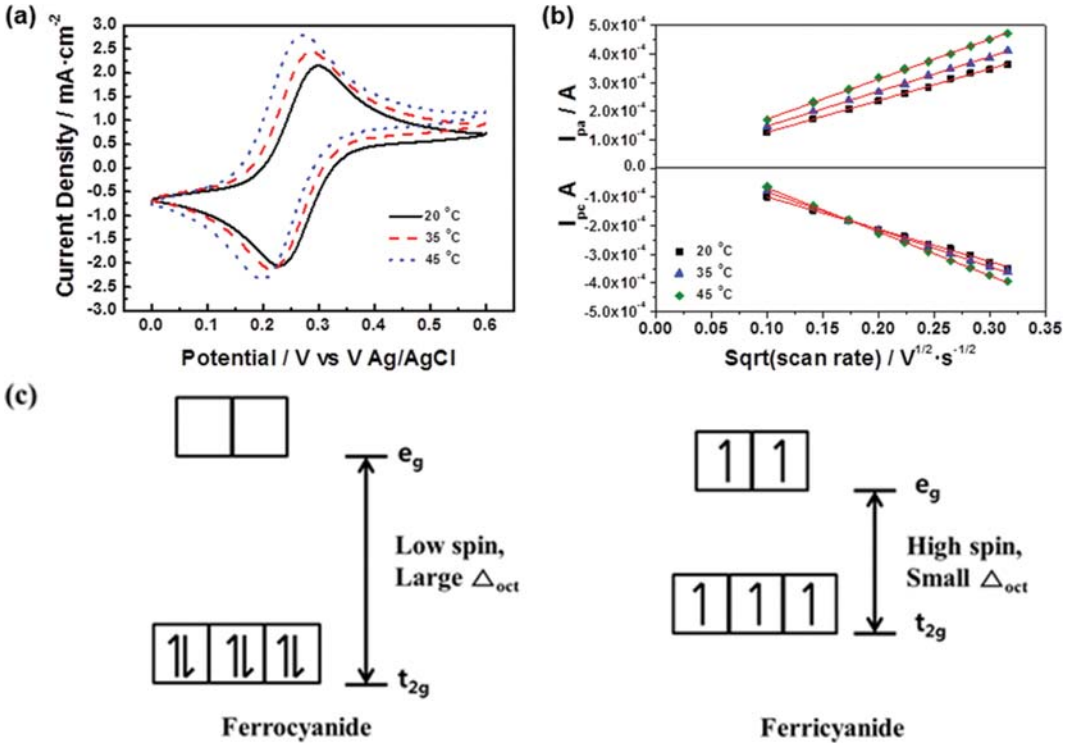

Fig. 2. (a) CV curves representing the redox reactivity of ferrocyanide and ferricyanide measured at different temperatures (20, 35 and 45 °C) with a scan rate of 100 mV s^{-1}, (b) peak current density versus square root of scan rate graphs for evaluating temperature effect on the redox reactivity of ferrocyanide and ferricyanide, and (c) schematics representing d orbital state of ferrocyanide and ferricyanide.

form of alloxazine-COOH is more stable than the pristine alloxazine-COOH in aqueous solution due to the hydrogen bonding stemming from the nitrogen element of alloxazine-COOH (Fig. 3(c)) [39]. In summary, as temperature increases, the reduction reaction rate of alloxazine-COOH significantly increases, while the oxidation reaction rate of that slightly increases [38].

2. The Performance of ARFB Full Cells

To evaluate the stability and performance of AORFB using allox-

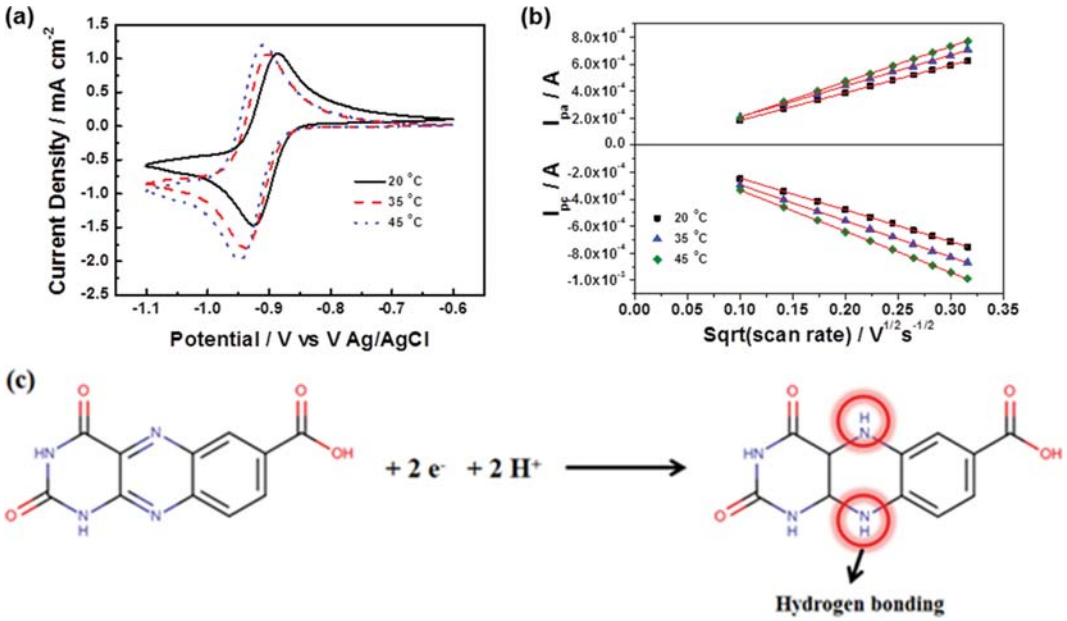

Fig. 3. (a) CV curves representing the redox reactivity of alloxazine-COOH measured in the different temperatures (20, 35 and 45 °C) with a scan rate of 100 mVs^{-1}, (b) peak current density versus square root of scan rate graphs for evaluating temperature effect on the redox reactivity of alloxazine-COOH, and (c) a schematic representing the reduction reaction of alloxazine-COOH.

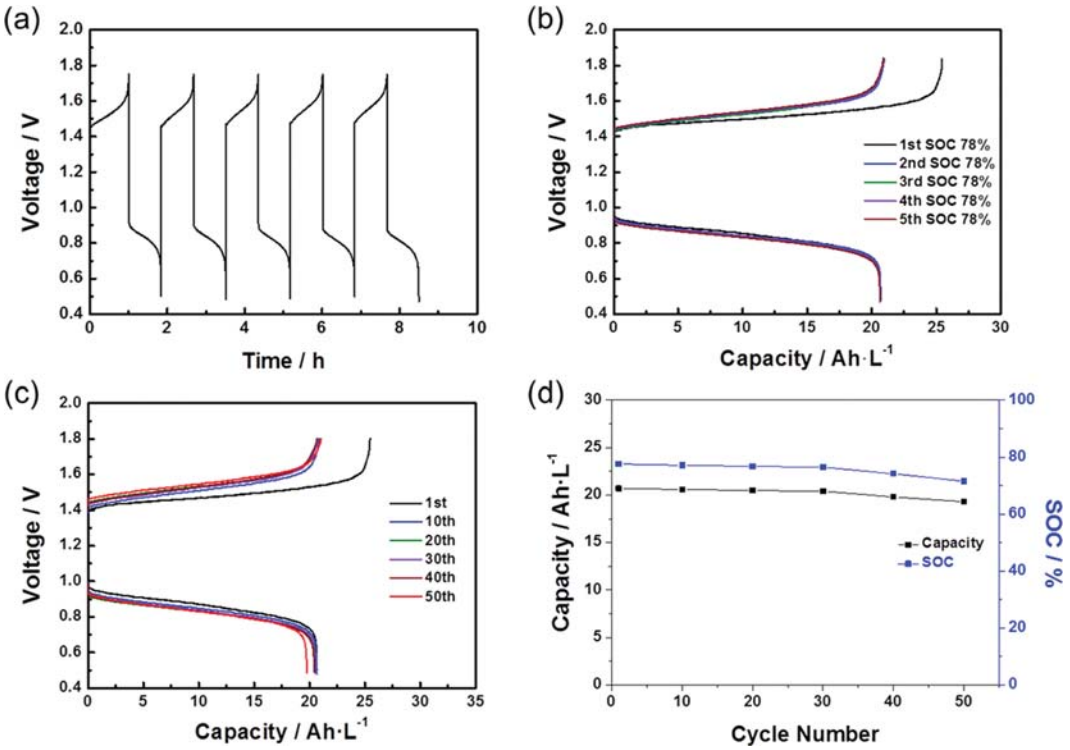

Fig. 4. (a) Voltage-time curves, (b) voltage-capacity curves at 1st-5th cycles, (c) voltage-capacity curves during cycling and (d) capacity or SOC graphs of AORFB single cell using 0.5 M alloxazine-COOH (15 mmol) under 2.5 M KOH 15 mL and 0.4 M ferrocyanide (45 mmol) under 1 M KOH 56.3 mL. Current density used was 100 $mA \cdot cm^{-2}$, while cut-off voltage range was 0.5-1.8 V.

azine-COOH and ferrocyanide at different temperatures, the effect of temperature on the performance of ARFB using the redox couple was measured. Initially, the ARFB full cell was run at 20 °C (room temperature). In that state, the average discharging capacity and state of charge (SOC) of ARFB measured during 50 cycle were 20.3 Ahr·L^{-1} and 76% (Fig. 4). After that, the performance of three different ARFB full cells - (i) only anolyte heated ARFB, (ii) only catholyte heated ARFB and (iii) both anolyte and catholyte heated ARFB - was measured.

Regarding "only anolyte heated AORFB" that was heated to 45 °C, when charge and discharge cycle tests were performed (Fig. 5), the time elapsed during the five cycles of ARFB single cell was 8.5 h and the starting charging and discharging voltages were 1.44 V and 0.92 V, while the average discharging capacity and SOC of ARFB single cell measured during 50 cycle were 22 Ahr·L^{-1} and 82%. In a comparison with the performance of ARFB single cell measured at 20 °C, the values obtained with only anolyte (ferrocyanide) heating increased a little, although this result did not match up with the electrochemical evaluation observed in Fig. 2.

According to the electrochemical characterization of ferrocyanide, its redox activity measured at 45 °C showed asymmetrical pattern, and due to the asymmetrical pattern, it is expected that the performance of "only anolyte heated ARFB" increases slightly more than that of non-heated ARFB. However, its actual ARFB perfor-

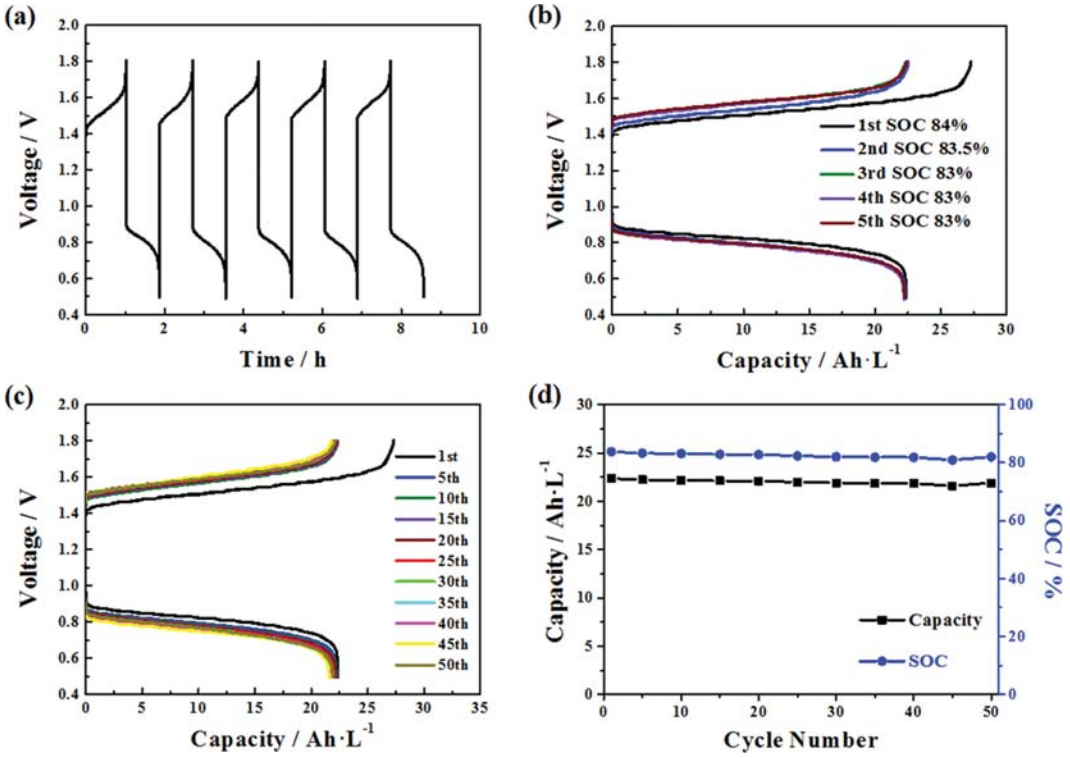

Fig. 5. (a) Voltage-time curves and (b) voltage-capacity curves measured for 1st-5th cycles of AORFB single cell. (c) Voltage-capacity curves of AORFB single cell measured during 50 cycle and (d) capacity or SOC graphs of AORFB single cell. All the tests were performed using 0.5 M alloxazine-COOH dissolved in 2.5 M KOH and 0.4 M ferrocyanide dissolved in 1 M KOH. Current density used was 100 mA·cm^{-2}, while cut-off voltage range was 0.5-1.8 V with only anolyte heating (ferrocyanide side). Heating temperature was 45 °C.

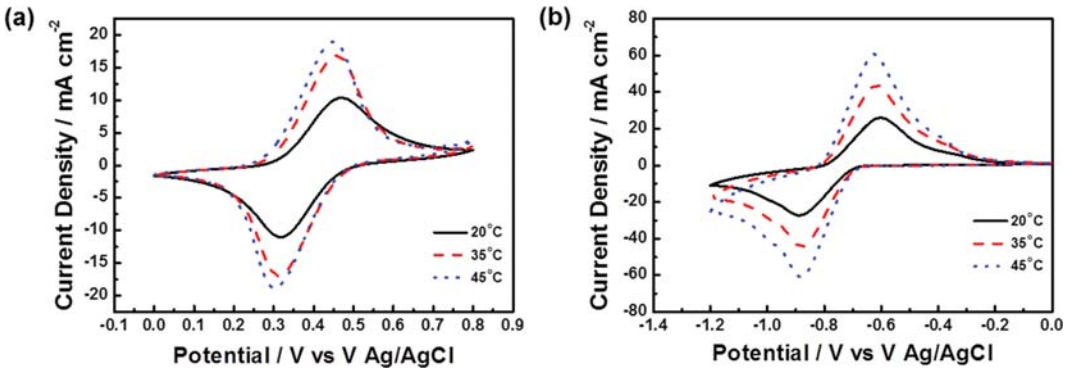

Fig. 6. CV curves representing the redox reactivity of (a) ferrocyanide and (b) alloxazine-COOH measured in the different temperatures (20, 35 and 45 °C) with a scan rate of 20 mVs^{-1}.

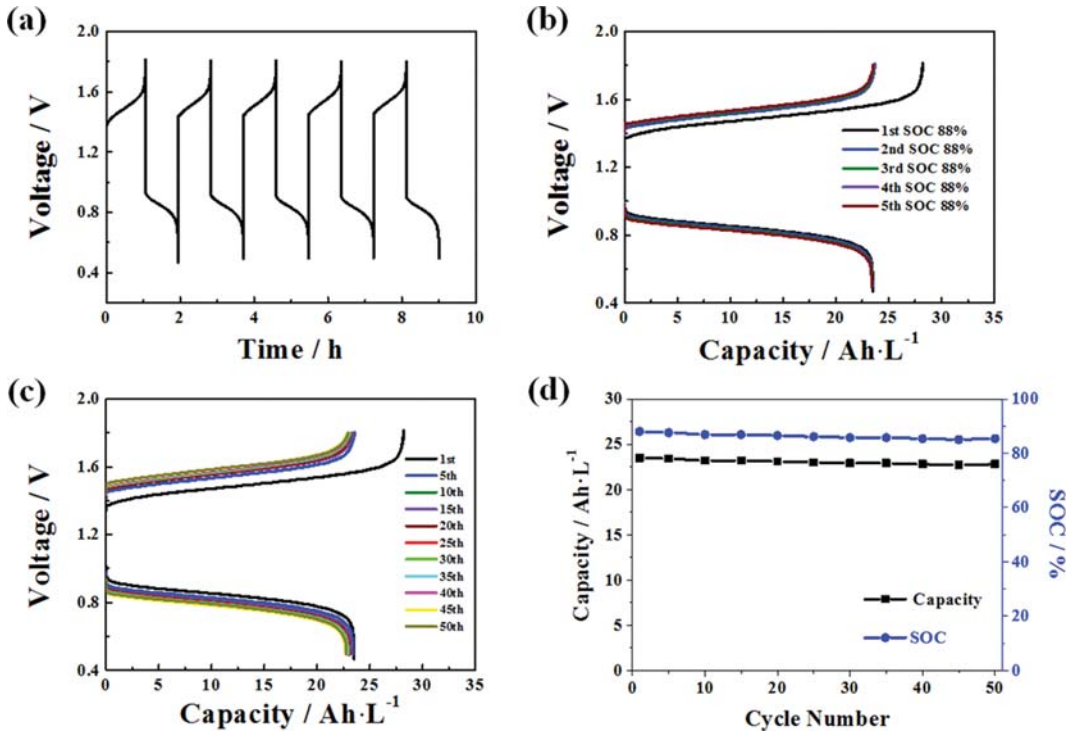

Fig. 7. (a) Voltage-time curves and (b) voltage-capacity curves measured for 1st-5th cycles of ARFB single cell. (c) Voltage-capacity curves of ARFB single cell measured during 50 cycle and (d) capacity or SOC graphs of ARFB single cell. All the tests were performed using 0.5 M alloxazine-COOH dissolved in 2.5 M KOH and 0.4 M ferrocyanide dissolved in 1 M KOH. Current density used was 100 mA·cm^{-2}, while cut-off voltage range was 0.5-1.8 V with only catholyte heating (alloxazine-COOH side). Heating temperature was 45 °C.

mance was more than expected. This result is partly due to the difference in electrode, meaning that GCE is used for half-cell tests, while carbon felt (CF) electrode is used for ARFB full cell tests. Unlike GCE, the CF contains functional groups like hydroxyl and carbonyl groups, which can improve the hydrophilicity of ferrocyanide that can affect its redox reactivity. To evaluate the effect of temperature on the electrochemical properties of ferrocyanide occurring onto the CF, its kinetic parameters were measured (Fig. 6(a)). In terms of electron transfer rate in the redox reaction of ferro/ferricyanide that is measured in different temperatures, the lower the anodic and cathodic peak potential difference is, the higher the electron transfer rate is. The potential peak difference of ferro/ferricyanide measured at 45 °C was 0.148 V, while the value measured at 20 °C was 0.152 V, meaning that the electron transfer rate was enhanced with elevated temperature. According to Fig. 6(a), with the use of CF, the redox reactivity of ferrocyanide was facilitated and occurred symmetrically. It is explained that the ferrocyanide/ferricyanide can exhibit a quasi-reversible electron-transfer kinetic onto the CF that has the carbon-oxygen terminal functional groups with hydrogen. Namely, the hydrophilic (charge-dipole) interaction between dipole groups (hydroxyl and carbonyl groups) onto the CF and ferricyanide ions promotes the oxidation reaction of ferricyanide, improving the asymmetric tendency of redox reaction of ferricyanide [40,41].

In Fig. 6(b), regarding electron transfer rate in the redox reaction of alloxazine-COOH that is measured in different temperatures, the lower the anodic and cathodic peak potential difference is, the higher the electron transfer rate is. The potential peak difference of alloxazine-COOH measured at 45 °C is 0.259 V, while the value measured at 20 °C is 0.286 V, meaning that the electron transfer rate was enhanced with elevated temperature.

Next, charge and discharge cycle tests of "only catholyte heated ARFB" were conducted; their charge/discharge curves are represented in Fig. 7. According to Fig. 7, "only catholyte heated ARFB" heated at 45 °C exhibited 9 h of charge-discharge time during the five cycles. In addition, the starting charging and discharging voltages were 1.42 V and 0.95 V, and the discharging capacity and SOC measured during 50 cycles were 23 Ahr·L^{-1} and 86%. In a comparison with the performance of ARFB single cell measured at 20 °C, the values increased a little, although this result did not match up with the electrochemical evaluation observed in Fig. 3.

According to the electrochemical characterization of alloxazine-COOH, its redox activity measured at 45 °C exhibited asymmetrical pattern. This is because the hydrophilic (dipole-dipole) interaction between dipole groups (hydroxyl and carbonyl groups) onto CF and dipole groups (nitrogen group) of alloxazine-COOH can activate the oxidation reaction of alloxazine-COOH [40-42]. This result leads to improvement in the performance of "only heated catholyte heated ARFB". In addition, according to our previous study, the redox reaction of alloxazine-COOH was a rate determining step (RDS), and thus for improving the performance of AORFB single cell, the redox reactivity of alloxazine-COOH should be enhanced. Therefore, the performance of "only catholyte heated ARFB" is further improved than that of "only anolyte heated ARFB" as temperature increases. It is proved that the reaction rate increases and the

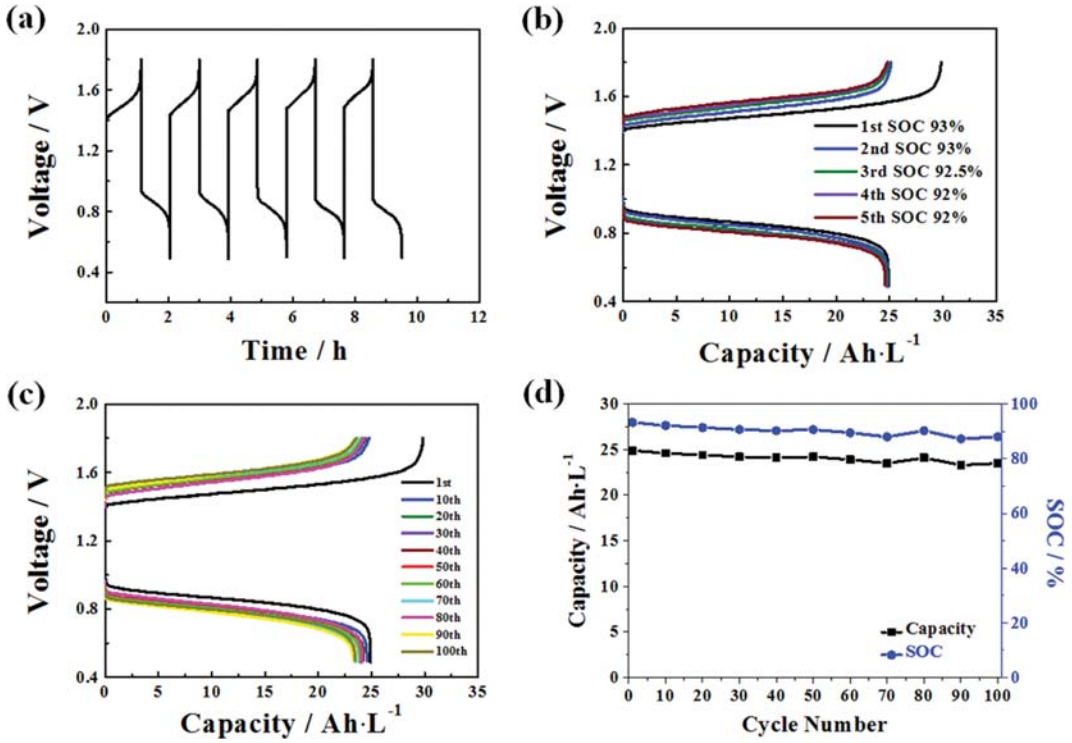

Fig. 8. (a) Voltage-time curves and (b) voltage-capacity curves measured for 1st-5th cycles of ARFB single cell. (c) voltage-capacity curves of ARFB single cell measured during 50 cycle and (d) capacity or SOC graphs of ARFB single cell. All the tests were performed using 0.5 M alloxazine-COOH dissolved in 2.5 M KOH and 0.4 M ferrocyanide dissolved in 1 M KOH. Current density used was 100 mA·cm^{-2}, while cut-off voltage range was 0.5-1.8 V with both anolyte and catholyte heating. Heating temperature was 45 °C.

kinetic energy of active species becomes higher than their activation energy with the increase in temperature.

Finally, for investigating heating impact on "both anolyte and catholyte heated ARFB", charge and discharge curves were measured (Fig. 8). According to Fig. 8, the ARFB exhibited 9.5 h of charge-discharge time during the five cycles. Furthermore, the starting charging and discharging voltages were 1.38 V and 0.99 V. Notably, the charging time of "both anolyte and catholyte heated ARFB" was much longer than that of "only anolyte heated ARFB" and "only catholyte heated ARFB". This means that as temperature increases, the solubility and kinetic energy of the two active species dissolved in aqueous solution increase. This indicates that as charging capacity, which is proportional to the solubility of active species, increases, the amount of available active species also increases during discharge, and finally, the discharging capacity and SOC increase (24.9 Ahr·L^{-1} and 93%).

Taken together, it is speculated that heating both alloxazine-COOH and ferrocyanide to 45 °C can be one solution for improving the performance of AORFB using alloxazine-COOH and ferrocyanide.

CONCLUSION

The effect of operating temperature on the performance of ARFBs using alloxazine-COOH and ferrocyanide as redox couple was evaluated. According to electrochemical characterizations, the redox reaction of ferrocyanide followed a quasi-reversible state at room temperature, and as temperature increased, the state became irreversible. To alleviate the irreversibility in redox reaction, CF electrode containing carbon-oxygen functional groups was effective. In case of the alloxazine-COOH, it preserved its reversible state relatively well, and its reduction activity increased with temperature due to the changes in polarity and hydrogen bonding capabilities occurring during redox reaction. This result could be explained that as temperature increased, the kinetic energy of the two active species also increased. The performance of ARFBs using them as redox couple was measured in the different temperature conditions. When the temperature of both anolyte and catholyte was 45 °C, average discharge capacity and state of charge were 24 Ahr·L^{-1} and 90%, and the values were best. In ARFB of only catholyte heating up to 45 °C, the values were reduced to 23 Ahr·L^{-1} and 86%, while ARFB of only anolyte heating up to 45 °C, they were reduced to 22 Ahr·L^{-1} and 82%. With this result, it is expected that the operation temperature is one of the important factors in deciding the performance of ARFB, and we believe that this result can provide important information for establishing commercial RFB system and be connected with other high temperature renewable energy systems, such as geothermal energy, because the extra heat produced from geothermal power can be used for effective charging this kind of ARFB system.

ACKNOWLEDGEMENT

This study was supported by the Research Program funded by the

SeoulTech (Seoul National University of Science and Technology).

REFERENCES

1. H. Chen, T. N. Cong, W. Yang, C. Tan, Y. Li and Y. Ding, *Prog. Nat. Sci.*, **19**, 291 (2009).
2. K.-J. Lee, S. Koomson and C.-G. Lee, *Korean J. Chem. Eng.*, **36**, 600 (2019).
3. S. Ghosh, S. M. Jeong and S. R. Polaki, *Korean J. Chem. Eng.*, **35**, 1389 (2018).
4. M. Christwardana, J. Ji, Y. Chung and Y. Kwon, *Korean J. Chem. Eng.*, **34**, 2916 (2017).
5. J. H. Ryu, *Korean J. Chem. Eng.*, **35**, 328 (2018).
6. M. Christwardana, Y. Chung and Y. Kwon, *Korean J. Chem. Eng.,* **34**, 3009 (2017).
7. M. Christwardana, Y. Chung, D. C. Tannia and Y. Kwon, *Korean J. Chem. Eng.*, **35**, 2421 (2018).
8. W. Wang, Q. Luo, B. Li, X. Wei, L. Li and Z. Yang, *Adv. Funct. Mater.*, **23**, 970 (2013).
9. A. Parasuraman, T. M. Lim, C. Menictas and M. Skyllas-Kazacos, *Electrochim. Acta*, **101**, 27 (2013).
10. H. Kaneko, K. Nozaki, Y. Wada, T. Aoki, A. Negishi and M. Kamimoto, *Electrochim. Acta*, **36**, 1191 (1991).
11. M. Jung, W. Lee, N. N. Krishnan, S. Kim, G. Gupta, L. Komsiyska, C. Harms, Y. Kwon and D. Henkensmeier, *Appl. Surf. Sci.*, **450**, 301 (2018).
12. C. Noh, M. Jung, D. Henkensmeier, S. W. Nam and Y. Kwon, *ACS Appl. Mater. Interfaces*, **9**, 36799 (2017).
13. W. Lee, C. Jo, S. Youk, H. Y. Shin, J. Lee, Y. Chung and Y. Kwon, *Appl. Surf. Sci.*, **429**, 187 (2018).
14. H. Y. Jung, M. S. Cho, T. Sadhasivam, J. Y. Kim, S. H. Roh and Y. Kwon, *Solid State Ion.*, **324**, 69 (2018).
15. I. Strużyńska-Piron, M. Jung, A. Maljusch, O. Conradi, S. Kim, J. H. Jang, H.-J. Kim, Y. Kwon, S.-W. Nam and D. Henkensmeier, *Eur. Polym. J.*, **96**, 383 (2017).
16. H. Y. Jung, S. Jeong and Y. Kwon, *Electrochem. Soc.*, **163**, A5090 (2016).
17. G. Oriji, Y. Katayama and T. Miura, *Electrochim. Acta*, **49**, 3091 (2004).
18. S. Jeong, L. H. Kim, Y. Kwon and S. Kim, *Korean J. Chem. Eng.*, **31**, 2081 (2014).
19. W. Wang, Z. Nie, B. Chen, F. Chen, Q. Luo, X. Wei, G.-G. Xia, M. Skyllas-Kazacos, L. Li and Z. Yang, *Adv. Energy Mater.*, **2**, 487 (2012).
20. M. H. Chakrabarti, R. A. W. Dryfe and E. P. L. Roberts, *Electrochim. Acta*, **52**, 2189 (2007).
21. M. Lopez-Atalaya, G. Codina, J. R. Perez, J. L. Vazquez and A. Aldaz, *J. Power Sources*, **39**, 147 (1992).
22. M. Zhang, M. Moore, J. S. Watson, T. A. Zawodzinski and R. M. Counce, *J. Electrochem. Soc.*, **159**, A1183 (2012).
23. C. Noh, S. Moon, Y. Chung and Y. Kwon, *J. Mater. Chem. A*, **5**, 21334 (2017).
24. C. Noh, C. S. Lee, W. S. Chi, Y. Chung, J. H. Kim and Y. Kwon, *J. Electrochem. Soc.*, **165**, A1388 (2018).
25. B. Li, M. Gu, Z. Nie, Y. Shao, Q. Luo, X. Wei, X. Li, J. Xiao, C. Wang, V. Sprenkle and W. Wang, *Nano Lett.*, **13**, 1330 (2013).
26. D. J. Suárez, Z. González, C. Blanco, M. Granda, R. Menéndez and R. Santamaría, *ChemSusChem*, **7**, 914 (2014).
27. Z. González, A. Sánchez, C. Blanco, M. Granda, R. Menéndez and R. Santamaría, *Electrochem. Commun.*, **13**, 1379 (2011).
28. B. Yang, L. Hoober-Burkhardt, F. Wang, G. S. Prakash and S. R. Narayanan, *J. Electrochem. Soc.*, **161**, A1371 (2014).
29. K. Lin, R. Gómez-Bombarelli, E. S. Beh, L. Tong, Q. Chen, A. Valle, A. Aspuru-Guzik, M. J. Aziz and R. G. Gordon, *Nature Energy*, **1**, 16102 (2016).
30. B. Hu, C. DeBruler, Z. Rhodes and T. L. Liu, *J. American Chem. Soc.*, **139**, 1207 (2017).
31. W. Lee, B. W. Kwon and Y. Kwon, *ACS Appl. Mater. Interfaces*, **10**, 36882 (2018).
32. J. Luo, A. Sam, B. Hu, C. DeBruler, X. Wei, W. Wang and T. L. Liu, *Nano Energy*, **42**, 215 (2017).
33. C. Zhang, T. S. Zhao, Q. Xu, L. An and G. Zhao, *Appl. Energy*, **155**, 349 (2015).
34. K. W. H. Stevens and M. H. L. Pryce, *Proc. R. Soc. Lond. A Math. Phys. Sci.*, **219**, 542 (1953).
35. W. T. Oosterhuis and G. Lang, *Phys. Rev.*, **178**, 439 (1969).
36. K. R. Dunbar and R. A. Heintz, *Prog. Inorg. Chem.*, **45**, 283 (1997).
37. M. Gembický, R. Boča and F. Renz, *Inorg. Chem. Commun.*, **3**, 662 (2000).
38. L. Bahadori, M. H. Chakrabarti, N. S. A. Manan, M. A. Hashim, F. S. Mjalli, I. M. AlNashef and N. Brandon, *PloS. One*, **10**, e0144235 (2015).
39. K. Nishimoto, Y. Watanabe and K. Yagi, *Biochim. Biophys. Acta Enzymol.*, **526**, 34 (1978).
40. K. J. Kim, S. W. Lee, T. Yim, J. G. Kim, J. W. Choi, J. H. Kim, M. S. Park and Y. J. Kim, *Sci. Rep.*, **4**, 6906 (2014).
41. M. M. Titirici and M. Antonietti, *Chem. Soc. Rev.*, **39**, 103 (2010).
42. S. Dutta Choudhury, J. Mohanty, A. C. Bhasikuttan and H. Pal, *J. Phys. Chem. B*, **11**4, 10717 (2010).